ELSEVIER

Surface Science 425 (1999) 31–47

surface science

Energetics and diffusion paths of gallium and arsenic adatoms on flat and stepped GaAs(001) surfaces

M.A. Salmi [a,*], M. Alatalo [b], T. Ala-Nissila [a,b,c], R.M. Nieminen [a]

[a] *Laboratory of Physics, Helsinki University of Technology P.O. Box 1100, FIN-02015 HUT, Espoo, Finland*
[b] *Helsinki Institute of Physics, P.O. Box 9, FIN-00014 University of Helsinki, Helsinki, Finland*
[c] *Department of Physics, Box 1843, Brown University, Providence, RI 02912-1843, USA*

Received 18 September 1998; accepted for publication 9 January 1999

Abstract

In this paper, we investigate the energetics and diffusion barriers of arsenic and gallium adatoms on smooth and stepped GaAs(001) surfaces. We use molecular-dynamics energy minimization with the Tersoff potential to calculate the adiabatic potential experienced by an adatom. For smooth surfaces, we consider the most stable structures that are important for molecular-beam epitaxy growth conditions. For these, we map out the potential surfaces and identify the diffusion paths over the lowest saddle points. In the case of stepped surfaces we consider the two simplest kinds of straight step, namely the A and B steps on the (001) surface. For gallium adatoms, we find evidence of a step-edge barrier for B steps, but no barrier for going down the A step, and no barriers for arsenic adatoms. The diffusion anisotropies along the two types of step edge are also estimated.

Keywords: Gallium arsenide; Low index single crystal surfaces; Models of surface kinetics; Molecular dynamics; Stepped single crystal surfaces; Surface diffusion; Surface relaxation and reconstruction

1. Introduction

Theoretical and experimental investigations of the surfaces and growth of gallium arsenide have been going on for some time [1]. The main reason for widespread interest towards this system are the electronic properties of GaAs surfaces, which suggest that fast microelectronic circuits could be manufactured using GaAs as a base. Typically, GaAs interfaces are grown by the molecular-beam epitaxy (MBE) technique [2]. In MBE, sources of elemental gallium and arsenic are heated, causing atoms to dissociate from the element surfaces, usually as gallium atoms and As_2 or As_4 molecules. Both species of atom then move to a substrate in a vacuum chamber, where they merge with the growing GaAs lattice. In an ideal case, the crystal lattice would grow smoothly, with few defects always exhibiting an atomically smooth surface. This would be especially desirable in the case of quantum dots and wires, where even small deviations from the level interface may destroy the unique electronic properties of the interface. Unfortunately, this kind of growth is hard to obtain. Growth conditions must be carefully controlled to avoid the formation of single-element clusters, usually consisting of gallium. Mounds or pyramid-like structures can also form on the surface. Although they can be smoothed by annealing

* Corresponding author. Fax: +358-9-451-3116; e-mail: matti.salmi@hut.fi.

0039-6028/99/$ – see front matter
PII: S0039-6028(99)00180-6

and other techniques, the optimal scheme would be to produce a relatively smooth surface from the beginning. Because of these reasons, both experimental [2–4] and theoretical [5–7] studies of MBE growth of GaAs are of great importance.

Following deposition of adatoms on the surface, the fundamental process that determines the growth properties of many materials under typical MBE conditions is surface diffusion. In the high-friction limit [8] adatoms are thermally activated and move along the adiabatic potential surface provided by the substrate. At low temperatures, diffusion is dominated by a path from the minimum on the potential to a nearby minimum via the lowest-energy saddle point [9]. According to the simple transition-state picture [10], the frequency of activated jumps follows an Arrhenius-type law: $\omega_0 = \omega_D \, e^{-E_D/k_B T}$, with ω_D being the frequency of small oscillations around the minimum in question and E_D the energy barrier between the minimum and the saddle point. The prefactor can also be estimated from the adiabatic potential using transition state theory (TST) [11].

Especially important for MBE growth are the potential near steps and the possible anisotropy in diffusion barriers in different directions. On the lower terrace near the step edge the potential surface minima may be lower than on the flat surface, causing the diffusing atoms to stick to the step edge. In addition to this, there may be different diffusion barriers in different directions along the edge. Also, on the higher layer above the step edge, there often is an additional step-edge energy barrier (the Erlich–Schwoebel barrier) [12,13], which hinders diffusion down from the higher terrace. This barrier causes the atoms to be reflected back to diffuse on the upper layer where they can merge to form islands and new layers [6]. This would result in partial layers forming on top of other partial layers, resulting in pyramid-like microscopic structures on the GaAs surface. This is, in fact, what is seen in experiments [3,4], at least at relatively low temperatures, and computer simulations [7]. This has been explained by an effective step-edge barrier for the diffusion of adatoms on the GaAs(001) surface [5,7].

The other effect suggested by experiments is the existence of diffusion anisotropy, especially along step edges. The edges parallel to the dimer direction (A-type steps) are usually hundreds of times longer than the edges perpendicular to the dimer direction (B-type steps) [14–16], as well as being smoother and straighter. When growth occurs on a vicinally cut substrate, which naturally has a higher concentration of steps to begin with, the growth occurring can be stable at the right growth conditions [17]. This is also an effect explained by the existence of a step-edge barrier.

In this paper, we present results from an extensive study of the diffusion characteristics of arsenic and gallium adatoms on the (001) surface of GaAs, motivated in part by its usefulness as a growth surface of quality crystals. Under MBE growth conditions, the surface is usually arsenic-terminated, while the actual growth of the GaAs structure is controlled mainly by the gallium flux. We estimate the adiabatic potential experienced by diffusing arsenic and gallium adatoms in order to understand the mechanism by which they move on the surface and incorporate into the lattice. For this, we minimize the surface energy with molecular dynamics (MD) methods using the empirical Tersoff potential [18]. Since evidence points to several different atomic configurations that may exist on the surface, we have first compared the different structures and reconstructions of the GaAs surface in order to determine the most stable ones under the conditions present in MBE growth, using our own results and information from other theoretical and experimental studies. After this, the adiabatic surface potentials for arsenic and gallium adatoms are mapped out for some of the most important structures. We also include two important step structures on the (001) surface, and study the energetics of adatoms in the vicinity of these steps. This is particularly interesting from the point of view of the observed growth instabilities on the (001) surface.

The outline of the paper is as follows. In Section 2, we first review of the structure and properties of the GaAs(001) surface. Results from theoretical and experimental studies on the growth and reconstructions are discussed. Section 3 explains the Tersoff potential used to model the interactions between atoms and the methods used to compare different surface structures. In

Section 4, the main results of the study are presented. The adiabatic surface potentials are calculated for several flat surface reconstructions [$\beta2(2\times4)$, $\beta(2\times4)$ and $c(4\times4)$] and two different types of surface step on the $\beta2(2\times4)$ reconstructed surface. The results are compared with those from other studies and their significance for growth is discussed. Finally, in Section 5 we summarize and discuss our results.

2. Properties of GaAs surfaces

2.1. Flat surface reconstructions

There is a large number of different reconstructions that have been reported on the GaAs(001) surface. These include the (4×4), (2×4), (2×8), (3×1), (1×6), (4×6), (4×1), (2×6), (4×2) and (8×2) structures, all of which have been discovered in different growth conditions [19–25]. Several of these have been suggested as being consistent with experimental data and theoretical arguments. The ones deemed most promising and studied in this work are shown in Fig. 1. The open circles show the positions of the arsenic atoms and the filled circles show the gallium atom positions. The size of the circle indicates its distance from the surface, with the largest circles being closest.

At the best growth conditions, the α and β phases of the (2×4) structure are seen. These have arsenic coverages of 0.5–0.75 monolayers. Simple energetic considerations [26] suggest that the atomic configuration of this structure cannot be explained by the dimer-row model evident on Si(001) surfaces. Instead, the simplest (2×4) configuration possible consists of three dimers in a row, separated by a single missing dimer (see Fig. 1b). The structures suggested for these (2×4) reconstructions are thus this three-dimer β configuration (Fig. 1b), as well as the α (Fig. 1a) and $\beta2$ (Fig. 1c) structures.

In addition to electron diffraction studies, experimental evidence for these structures comes from scanning tunneling microscope (STM) studies of GaAs(001) surfaces [27]. Structures measuring 8 Å by 16 Å have been observed, corresponding to a (2×4) surface cell on the GaAs(001) surface. The structure of the cell also seems to correspond

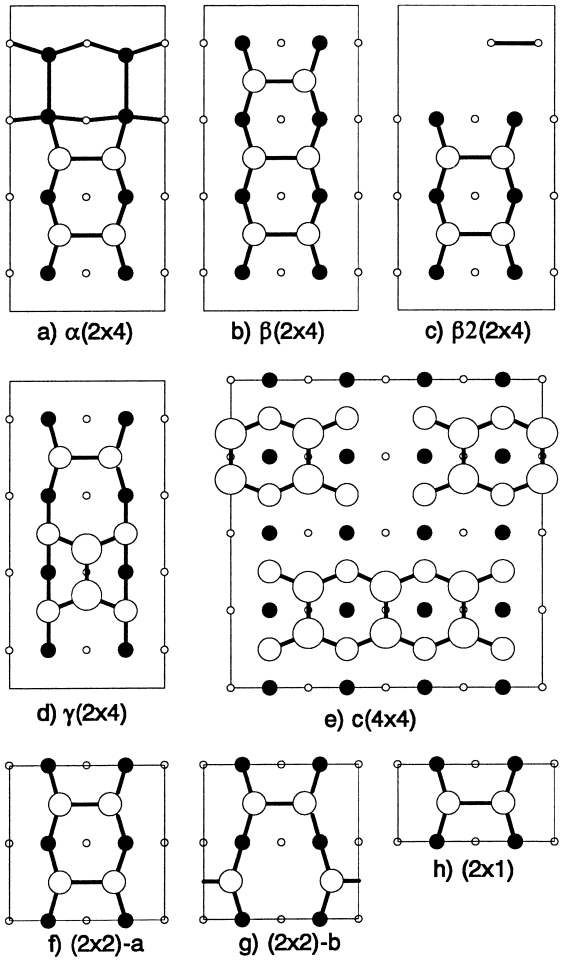

Fig. 1. The most important surface structures for GaAs(001). Open circles designate arsenic atoms and filled circles gallium atoms.

to the β structure suggested [26]. A structure commonly observed in these STM images was a single surface cell (4 Å) shift in the short-edge direction at the missing dimer position. This would explain the (2×8) symmetry [28] observed in some reflection high-energy electron (RHEED) measurements. Other STM images [29–34], made of surfaces grown in slightly different conditions, have also detected a (2×4) structure that seems to consist of two dimers and two missing dimers, which also appears to be a stable structure in some cases. This may signify either an α or a $\beta2$ structure.

Somewhat higher arsenic fluxes during growth result in the γ phase, with a single monolayer coverage. The simplest dimer reconstruction would be a (2×1) surface with long dimer rows (Fig. 1h), which is unlikely for GaAs. Instead, it has been suggested that the γ phase would also have a (2×4) symmetry, with the configuration seen in Fig. 1d. This was also found to be energetically favorable to the unreconstructed and the dimerized (2×1) surface in ab initio calculations [35]. Subsequent theoretical calculations [36] have suggested that there are large periodic structures which are more stable. The study of these structures was motivated by observed (8×7) reconstructions in STM/RHEED studies [29], and therefore the experimental and theoretical evidence both point to a stable (8×7) surface under some growth conditions.

At even higher arsenic fluxes, the $c(4\times4)$ structure is observed. Early RHEED and photoemission studies [37] suggested a configuration consisting of arsenic dimers on top of a relatively unreconstructed arsenic layer. More recent studies [38] have shown that the most common structure observed has a 1.75 monolayer coverage, consisting of three-dimer groups (Fig. 1e). This is also commonly observed in STM images [39]. This type of structure is also seen after annealing the (2×4) surface at high arsenic pressures.

Existing theoretical studies support these reconstructions, too. Ohno [40] studied several structures with different arsenic coverages. He found that the lowest-energy structure at very high arsenic pressures was the $\gamma(2\times4)$ configuration, but for most of the acceptable arsenic pressures, the lowest-energy structures are the $\beta(2\times4)$ or $\beta(2\times8)$ configurations (with an energy difference of less than 0.005 eV per surface cell), with the β2 surface only 0.02 eV above it. Northrup and Froyen [35,41] used a similar technique and found the $c(4\times4)$ surface dominating in high arsenic pressures, followed by the $\beta2(2\times4)$ and then the $\alpha(2\times4)$ surfaces at somewhat lower pressures, and finally the gallium-terminated $\beta2(4\times2)$ surface. In [35] it was also noted that a simple calculation of the Madelung energies of the surfaces seems to give a remarkably accurate estimate of the energy differences of the various surfaces as compared with the ab initio studies, always yielding the correct signs and magnitudes for the energies. This suggests that the simple electrostatic interactions may be the key component in determining the stability of the structures.

2.2. Surface steps

Under practical MBE growth conditions, all surfaces of the growing GaAs(001) surface are arsenic-terminated, and consequently all step structures are between two arsenic-terminated surfaces. The possible steps can be oriented in different directions with respect to the surface dimers. This gives rise to a large number of possible steps, whose stability must be determined. Zhang and Zunger [42] have proposed a simplified method called linear combination of structural motifs (LCSM), which gives reasonable agreement with other calculations of simpler structures, and has been used to calculate the energies of complicated structures, including surface steps. For our study, we have chosen those simple steps that were found to have the lowest energies in the LCSM study. It should be noted that the LCSM study concluded that these simple step structures would not be stable, but proposed that the actual steps would have to have some sort of stabilizing defects. Despite this, we have calculated the surface potential only for the simple steps, since the number of possible charge-balancing defects on a step edge is huge.

The A type of step with the lowest energy has the configuration shown in Fig. 2. In the A step structure, the steps form parallel to the short edge of the (2×4) reconstruction, in the direction of the top arsenic dimers. Similarly, the B-type step with the lowest energy is shown in Fig. 3. In the B step structure, the steps form parallel to the long edge of the (2×4) reconstruction, perpendicular to the direction of the top-layer arsenic dimers.

3. Methods

3.1. Model for interaction potential

We shall study the surface properties by calculating the energies of the different surface configurations, using molecular dynamics (MD)

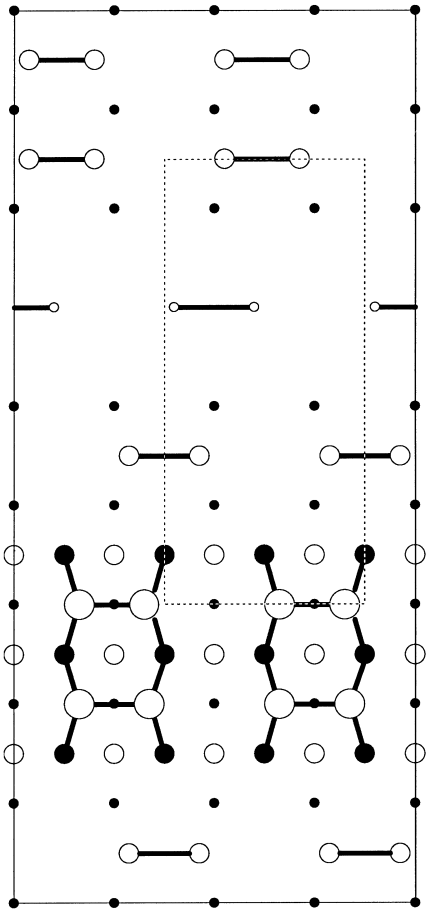

Fig. 2. The structure of the A-β2(2×4) step. Open circles designate arsenic atoms and filled circles gallium atoms.

calculations and the empirical Tersoff potential to model the interactions between gallium and arsenic atoms and periodic boundary conditions in the direction of the surface.

In the Tersoff formulation [18,43], the total potential energy of the system is

$$V=\frac{1}{2}\sum_{i\neq j} f_{\mathrm{C}}(r_{ij})[V_{\mathrm{R}}(r_{ij})-B_{ij}V_{\mathrm{A}}(r_{ij})]. \tag{1}$$

Since the main contribution to potential energy comes from nearest neighbors, the potential is modified with a smooth cutoff function f_{C}, which allows the potential to decrease gradually to zero in the vicinity of the cutoff distance R (in this case, in the range 3.4–3.6 Å).

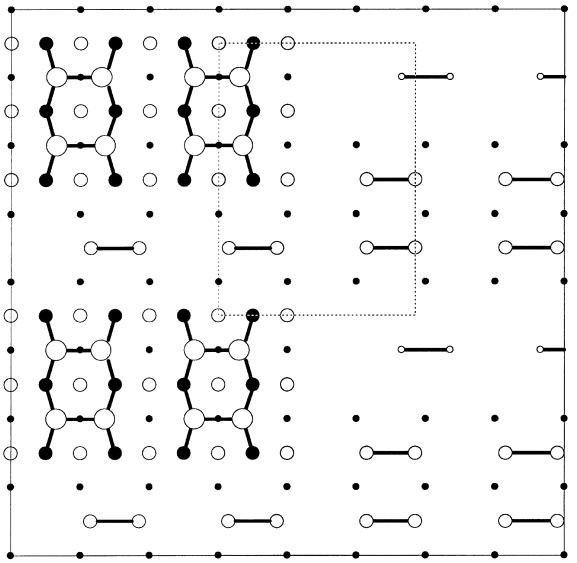

Fig. 3. The structure of the B-β2(2×4) step. Open circles designate arsenic atoms and filled circles gallium atoms.

The potential itself contains a repulsive and an attractive part, V_{R} and V_{A}, that both have the exponential, Morse-type form

$$V_{\mathrm{R}}(r)=A\,\mathrm{e}^{-\lambda_1 r} \tag{2}$$

$$V_{\mathrm{A}}(r)=B\,\mathrm{e}^{-\lambda_2 r}. \tag{3}$$

Beginning from the assumption that the number of neighbors should affect the strength of a single bond, weakening the interaction as the number of bonds increased, Tersoff added a term to modify the attractive potential V_{A}. This function B_{ij} is given by the equation

$$B_{ij}=(1+\beta^n\xi_{ij}^n)^{-1/2n}, \tag{4}$$

where

$$\xi_{ij}=\sum_{k\neq i,j} f_{\mathrm{C}}(\boldsymbol{r}_{ik})g(\theta_{ijk})\,\mathrm{e}^{\lambda_3^3(r_{ij}-r_{ik})^3}, \tag{5}$$

$$g(\theta_{ijk})=1+\frac{c^2}{d^2}-\frac{c^2}{d^2+(h-\cos\theta_{ijk})^2}. \tag{6}$$

Here B_{ij} measures the relative strength of the attraction between atoms i and j, which depends on the parameters β and n, and the function ξ_{ij}, which measures the total effect of all nearby atoms on the interaction. The cutoff function f_{C} is again used to remove the effect of the more distant atoms

from the calculation and the angular positions of the atoms are modelled with the function $g(\theta_{ijk})$ where θ_{ijk} is the angle between atoms j and k, measured from atom i, and the parameters c, d and h are determined through fitting to experimental data.

Tersoff's potential was developed to describe the interactions in elemental semiconductors. It was later expanded to cover compound materials [44], using a single parameter to combine the potentials of the components into a single interaction potential.

In this paper, we have used a potential [45] which explicitly states the potential parameters for Ga–Ga, Ga–As and As–As interactions. We have used the slightly altered parameters given by Sayed et al. in [46].

Table 1 gives Sayed's potential parameters for Ga–Ga, As–As and Ga–As interactions. These parameters were fitted especially to accurately model small arsenic clusters and GaAs dimers [45] as well as bulk properties, which makes this potential a reasonable choice for modelling the behavior of near-surface arsenic dimers.

3.2. Total energies of surfaces

To compare the energetics of surfaces in different chemical environments, we use the method outlined in [41] and used in studies of GaAs surfaces [40,41,47]. To this end, first the total energy U of the surface configuration is calculated. The total surface energy of a given structure is

$$\Omega = U - n_{\mathrm{Ga}}\mu_{\mathrm{Ga}} - n_{\mathrm{As}}\mu_{\mathrm{As}}, \tag{7}$$

where n_{As} and n_{Ga} are the number of arsenic and gallium atoms, respectively, in the simulation cell and μ_{As} and μ_{Ga} are their chemical potentials.

In addition, equilibrium with the bulk phase of GaAs requires that the sum of the chemical potentials equals the bulk energy; i.e., $\mu_{\mathrm{As}} + \mu_{\mathrm{Ga}} = E_{\mathrm{GaAs,bulk}}$. By using this constraint, the surface energy Ω can be written as a function of a single variable:

$$\Omega = U - n_{\mathrm{Ga}}E_{\mathrm{GaAs}} - (n_{\mathrm{As}} - n_{\mathrm{Ga}})\mu_{\mathrm{As}}. \tag{8}$$

On the other hand, the chemical potentials are also constrained by the energies of bulk arsenic and gallium ($\mu_{\mathrm{Ga(As)}} \leq \mu_{\mathrm{Ga(As),bulk}}$). The energies of bulk arsenic and gallium, $\mu_{\mathrm{Ga(As),bulk}}$, can also be calculated with the MD program. These constrain the possible chemical potential μ_{As} in MBE growth.

To study the diffusion of arsenic and gallium adatoms on the GaAs surface, we have to find out the adiabatic potential that acts on the adatom, as defined for example in [8]. A good approximation of the potential can be obtained by using the scheme outlined in [48]. An adatom is placed above the reconstructed surface in the xy plane. It is kept stationary, while the surface atoms are allowed to relax in the direction of the forces between them and the adatom. No thermal motion is allowed, and the forces eventually become negligible as the atoms reach new equilibrium positions. After relaxation the total energy of the system is recorded and the adatom is moved closer to the surface. The relaxation procedure is repeated several times, giving the energy as a function of adatom height. The minimum of this function is the potential at these coordinates in the xy plane. After finding the potential in one point in the xy plane, the procedure is repeated at the next x and y coordinates, until the whole surface cell has been mapped with acceptable resolution. This gives the potential experienced by the adatom in question at $T=0$, which can be used to estimate the diffusion characteristics.

Table 1
Tersoff potential parameters for GaAs. From [46]

	As–As	Ga–Ga	Ga–As
A (eV)	1571.86084	993.888094	2543.2972
B (eV)	546.4316579	136.123032	314.45966
λ_1 (Å^{-1})	2.384132	2.508427	2.8280926
λ_2 (Å^{-1})	1.728726	1.49082	1.72301158
λ_3 (Å^{-1})	1.729	1.490824	1.723
β	0.00748809	0.23586237	0.357192
n	0.60879133	3.4729041	6.317410
c	5.2731318	0.07629773	1.226302
d	0.75102662	19.796474	0.790396
h	0.15292354	7.1459174	−0.518489

4. Results

4.1. Total energies and stable structures for flat surfaces

First, we compare the possible atomic structures to determine the most stable configurations, as was done in the ab initio studies [40,41]. For this, we have taken the most likely candidates for the arsenic-terminated (2×4) cell, at different arsenic coverages: the α, β, β2 and γ configurations. Some unlikely surface structures, such as the unreconstructed surface and reconstructed (2×1) dimer row model, were also calculated for comparison and evaluation of the dimerization energy. For even higher arsenic coverages, the $c(4\times4)$ configuration with a 1.75 monolayer arsenic coverage was used. Although the gallium-terminated surfaces are not usually evidenced in MBE growth, the gallium-terminated (4×2) configurations α, β and β2, as well as the $c(2\times2)$ surface, were also considered.

The MD simulation cell used in the calculation was four bulk lattice cells thick (22.6 Å) and had an area of (8×8) surface cells (32 Å × 32 Å) and periodic boundary conditions were used in the directions parallel to the surface. The surface atoms were first placed in the positions suggested by earlier studies and allowed to relax in the direction of the forces acting on them until the energy of the system reached its equilibrium value. The numerical accuracy of the adiabatic potentials in our study is 0.01 eV as determined from the convergence of the calculations. At best then our barriers would have an accuracy of 0.02 eV, in addition to the possible inaccuracies of the potential parameters.

In addition, to find the range of μ_{As} limited by the bulk phases of arsenic, gallium, and GaAs, we must calculate the energies of the bulk forms of these materials. For bulk GaAs, this calculation gives an energy of 3.25 eV per atom. Bulk gallium was calculated to have an energy of 3.03 eV per atom, while bulk arsenic had an energy of 2.82 eV per atom. These energies are the bulk phase values of the chemical potentials $\mu_{Ga,bulk}$ and $\mu_{As,bulk}$, which constrain the effective chemical potentials, along with the requirement that $\mu_{As}+\mu_{Ga}=E_{GaAs}$, which can also be stated using the formation energy, ΔH_f: $E_{GaAs}=\mu_{Ga,bulk}+\mu_{As,bulk}+\Delta H_f$. The combination of these constraints leads to μ_{As} being constrained to the range $\mu_{As,bulk}-\Delta H_f \le \mu_{As} \le \mu_{As,bulk}$. Using the calculated bulk energies, this gives the range 2.17 eV $\le \mu_{As} \le$ 2.82 eV. The formation energy ΔH_f is 0.65 eV, somewhat lower than experimental results (0.83 eV [49]) or ab initio calculations (Northrup and Froyen [50]: 0.92 eV, Ohno [40]: 0.74 eV). Thus, it is possible that the allowed potential range is actually larger, but even a somewhat wider range would not introduce new candidates for the lowest-energy reconstruction.

The resulting energies, in electron volts per (1×1) surface cell, are shown in Fig. 4 as a function of μ_{As}, which has been shifted so that the zero of the potential in the figure equals the bulk arsenic value, $\mu_{As,bulk}$. For most of the allowed range, the $c(4\times4)$ surface with a 1.75 monolayer arsenic coverage has the lowest energy. This agrees with Northrup and Froyen's ab initio calculations [41]. This reconstruction is also often seen in experiments performed under conditions of high arsenic flux and relatively low temperatures.

With increasing μ_{As}, we observe a region of stability for the γ surface with a single monolayer coverage. It has the same stoichiometry as the (2×1) dimer-row structure, which is constantly only 0.014 eV/(1×1) above the γ surface energy, which is likely to be much less than the accuracy

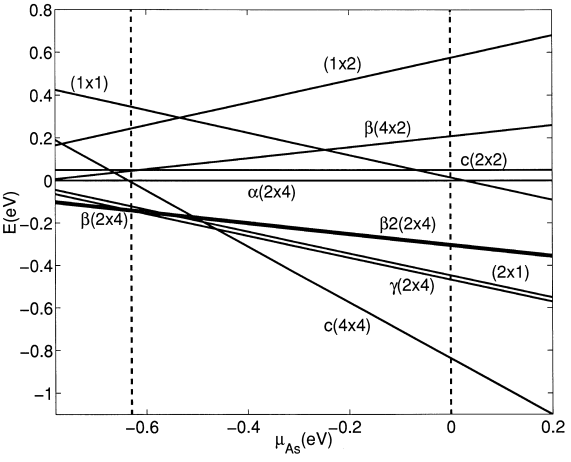

Fig. 4. Surface energies of the various reconstructions.

Table 2
Energy differences ΔE between configurations with the same stoichiometry, in units of eV/(1×1) cell. The last two colums show results from other works

As coverage	Most stable	Other structure	ΔE	ΔE [50]	ΔE [40]
1.0	$\gamma(2\times4)$	(2×1)	0.014	–	–
		unreconstructed	0.47	–	–
0.75	$\beta(2\times4)$	$\beta2(2\times4)$	0.008	−0.05	0.02
0.5	$\alpha(2\times4)$	$c(2\times2)$	0.05	0.05	–
0.25	$\beta(4\times2)$	$\beta2(4\times2)$	0.001	−0.03	–

of our results. Increasing μ_{As} further, we find the next stable structure, the β surface, which has an energy of 0.008 eV/(1×1) lower than the β2 surface. Similar results were reported by Ohno [40], whose ab initio calculations agree with our results, in contrast to Northrup and Froyen [35], who predicted that the β2 would be the most stable structure.

This information can also be stated as energy differences between surfaces of different stoichiometry, as shown in Table 2 as electron volts per (1×1) surface cell, with comparison to other calculation results. For each coverage, the energies of other structures are compared with the most stable structure according to our calculations.

The energy differences between different surfaces are small for all calculations[1]. This is most clearly seen in our MD simulations, which give smaller differences than either of the ab initio calculations. Like Ohno [40], we find the β surface to be the most stable, for both the arsenic- and gallium-terminated cases, but our energy differences are much smaller, in the meV range.

In Table 3 we compare our results for the length of the surface arsenic dimer bonds with other studies. In the table, ab initio refers to various pseudopotential calculations and MD to molecular dynamics simulations with various semi-empirical potentials. Experimental methods include RHEED, X-ray scattering (XS), X-ray photoelectron diffraction (XPD), energy-dependent photoelectron diffraction (EDPD), medium-energy ion scattering (MEIS) and secondary-ion mass spectroscopy (SIMS). For comparison, the bond length of nearest neighbors in bulk arsenic is 2.52 Å. The latest ab initio studies for $\beta/\beta2(2\times4)$ surfaces seem to indicate surface arsenic dimer lengths in the range of 2.5 Å to 2.6 Å.

The results obtained by the present MD studies give surface arsenic dimer lengths in excess of most experimental and theoretical results. The differences are most noticeable in the case of ab initio calculations. This may be partially explained by the use of the local density approximation which is known to give bond lengths that are shorter than the actual ones, at least in bulk calculations. Even then, the differences are usually under 10%.

The results of our calculations (Fig. 4) suggest that the most interesting structures for growth would seem to be the $\beta(2\times4)$ and $\beta2(2\times4)$ surfaces, which are very close in energy, as they are in ab initio studies and the $c(4\times4)$ structure. The adiabatic potential surfaces are therefore calculated for these surface reconstructions, for both arsenic and gallium adatoms. In addition, the potential surfaces for two simple perpendicular step structures (A and B) on a surface exhibiting the $\beta2(2\times4)$ reconstruction are calculated.

4.2. Adiabatic potentials for flat surfaces

For the mapping of the adiabatic potential surface, an orthogonal mesh with a 0.25 Å spacing in the x and y directions was used. The figures below describe the potential surface of the smallest possible surface cell, in most cases the (2×4) cell, calculated for both an arsenic and a gallium adatom. The potential surfaces for all reconstruc-

[1] In our calculations, the energy difference between the unreconstructed and the dimerized (2×1) surfaces comes to 0.91 eV per dimer, in comparison with 0.7 eV calculated by Qian et al. [51] in their early ab initio calculations.

Table 3
Comparison of theoretical and experimental estimates of surface arsenic dimer lengths, as compared with the present work

Dimer length (Å)	Method	Surface	Maximum difference (%)	Reference
2.89 ± 0.1	MEIS	(2×4)	10.3	[52]
2.2–2.6	RHEED	(2×4)	18.8	[53]
2.48 ± 0.2	RHEED	(2×4)	15.9	[54]
2.73 ± 0.10	SIMS	(2×4)	3.0	[55]
2.9	STM	(2×4)	7.0	[56]
2.8	STM	(2×4)	3.3	[57]
2.50–2.52	ab initio	(2×4)	7.7	[58]
2.45–2.50	ab initio	(2×4)	9.6	[47]
2.4	EDPD	$c(2\times8)/(2\times4)$	11.4	[59]
2.2 ± 0.2	XPD	$c(2\times8)/(2\times4)$	26.1	[60,61]
2.60	ab initio	$\beta(2\times4)$	4.1	[62]
2.53	ab initio	$\beta2(2\times4)$	6.6	[50]
2.50	ab initio	$\beta2(2\times4)$(top)	7.7	[63]
2.61	ab initio	$\beta2(2\times4)$(3rd)	3.7	[63]
2.71	MD (Tersoff)	$\beta2/\beta(2\times4)$(top)	0	present
2.69 ± 0.10	SIMS	$c(4\times4)$	6.5	[55]
2.56–2.62	XS	$c(4\times4)$	4.3	[38]
2.62–2.67	MD (Tersoff)	$c(4\times4)$(top)	0	present

tions are presented in the same format. In all cases, the adiabatic potential energy is measured in eV in comparison to the situation where the adatom is infinitely far away and the surface structure is unperturbed. Therefore, the largest negative energies in the figures signify the deepest minima. The surface coordinates are reported in Å. The relaxations in the surface due to the presence of an adatom are generally in the range 0.1–0.3 Å. On the average, an adatom in the equilibrium position is 0.1–0.2 Å above the original position of the highest surface atoms. The calculated potentials and their minima and saddle points are shown in contour plots together with the surface arsenic shown as empty circles for arsenic atoms, and gallium atoms as filled circles, and nearest-neighbor bonds depicted by dark lines. The size of the circles indicates their proximity to the surface.

The potential surface experienced by an arsenic adatom over the $\beta2(2\times4)$ surface is shown in Fig. 5 and in Fig. 6 for a gallium adatom. Table 4 shows the energy values of the minima and saddle points. For the $\beta(2\times4)$ surface, Figs. 7 and 8 show the potential surfaces for the arsenic and gallium adatoms, respectively, and Table 5 contains the minima and saddle points. Finally, for the $c(4\times4)$ surface, the potential surface for the arsenic adatom is depicted in Fig. 9 and for the gallium adatom in Fig. 10. Table 6 shows the minima and saddle points.

For an arsenic adatom on a $\beta(2\times4)$ surface, the lowest minima are located directly in the middle of the surface arsenic dimer. This is also the case for the potential for a gallium adatom, for which the potential surface around the minima also seems to be less steep, which indicates a lower oscillation frequency. For the $\beta(2\times4)$ surface, the minima are approximately in line with the surface arsenic dimers, at the short-bridge sites as before. The potential surface for arsenic is again steeper than the surface for gallium. For the $c(4\times4)$ reconstruction, the minima are located between two surface arsenic dimers in the three-dimer grouping.

For the flat surfaces, the main diffusion energy barriers E_D have been collected in Table 7. It can be seen that, for the (2×4) surfaces, the results support a varying diffusion bias in the favor of the $(\bar{1}10)$ direction; i.e., in the direction of the surface dimers. In most cases, the bias is not very large, and for the $c(4\times4)$ surface, the diffusion bias is in the opposite direction. This is, however,

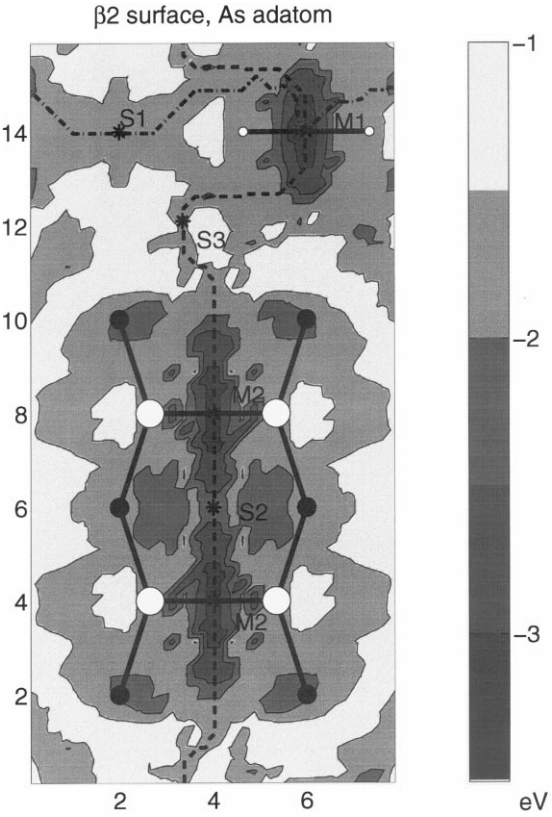

Fig. 5. The surface potential (with minima, saddle points and main diffusion paths) of the β2(2×4) reconstruction for an arsenic adatom.

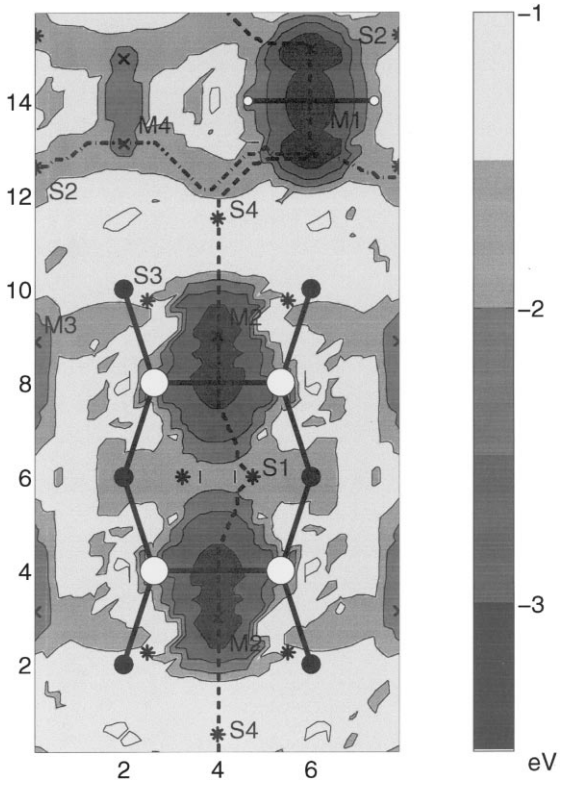

Fig. 6. The surface potential (with minima, saddle points and main diffusion paths) of the β2(2×4) reconstruction for a gallium adatom.

the direction of the arsenic dimers of the c(4×4) surface, meaning that diffusion is still biased in the direction of the surface arsenic dimers.

There have been some other recent attempts to map the potential surface for the GaAs(001) surface. For the β/β2(2×4) surfaces, ab initio calculations have been done for cation adatoms. In order to understand the formation of GaAs and GaAlAs heterostructures, Ohno et al. [64] calculated the diffusion constants for both gallium and aluminum adatoms on GaAs(001) exhibiting the three-dimer β(2×4) reconstruction. For the gallium adatom they found that the absolute minimum was located on a long-bridge site, in line with the surface arsenic dimers, but directly between them. The absolute minimum was located between middle dimers and the second lowest site was between the edge dimers of the three-dimer group. In the present work, minima are also found at the long-bridge site, but they are 0.8–1.0 eV higher in energy than the absolute minima at the short-bridge sites.

Table 4
Minima and saddle points on the β2(2×4) surface

	Label	Energy (eV)	
		As	Ga
Minima	M1	−3.13	−3.35
	M2	−3.06	−3.26
	M3	–	−2.43
	M4	–	−2.45
Saddle points	S1	−1.60	−1.83
	S2	−2.16	−1.65
	S3	−1.53	−1.45
	S4	–	−1.25

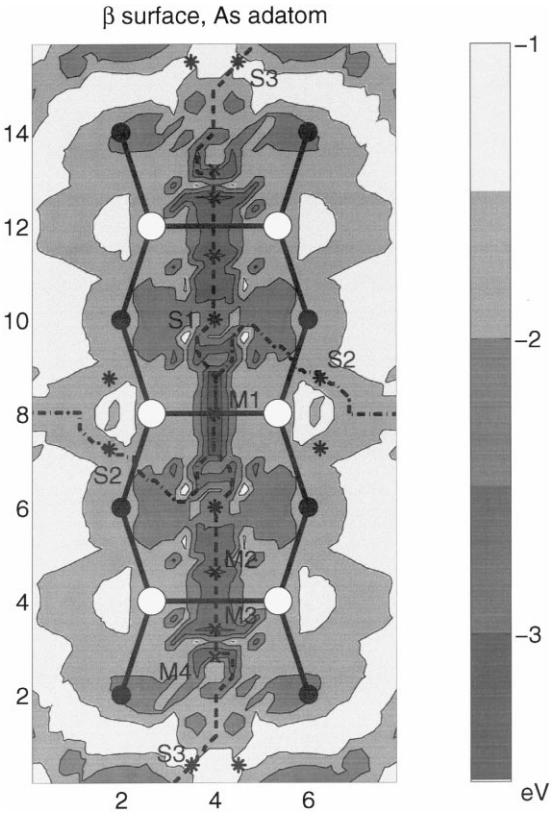

Fig. 7. The surface potential (with minima, saddle points and main diffusion paths) of the β(2×4) reconstruction for an arsenic adatom.

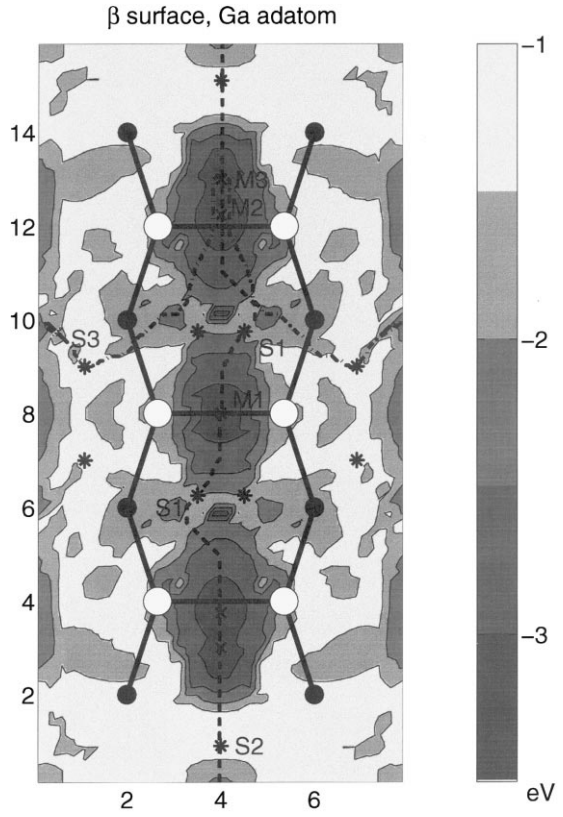

Fig. 8. The surface potential (with minima, saddle points and main diffusion paths) of the β(2×4) reconstruction for a gallium adatom.

A similar study for the β2(2×4) was done by Kley and Scheffler [65]. They found that if the surface atoms were not allowed to relax and especially the arsenic dimers were not allowed to break apart, the lowest minima were found on the long-bridge sites between the top-layer arsenic dimers as well as the exposed lower-layer dimer. In that case, their results were similar to those of Ohno et al. [64]. However, if the surface atoms were allowed to relax freely, the lowest minima were found on short-bridge sites, in line with the arsenic dimers, but directly between the surface arsenic atoms, as was also found in the present work.

Similarly, the MD calculations of Matthai and Moran [66] for the β(2×4) surface, which used the same formulation of the Tersoff potential as was used in this paper, also found that the lowest-energy minima are at the short-bridge sites, for both gallium and arsenic adatoms. They report no diffusion anisotropy.

Table 5
Minima and saddle points on the β(2×4) surface

	Label	Energy (eV)	
		As	Ga
Minima	M1	−3.10	−3.14
	M2	−3.05	−3.13
	M3	−3.03	−3.29
Saddle points	S1	−1.63	−1.82
	S2	−1.61	−1.28
	S3	−1.50	−1.42

Thus, although the Tersoff potential has been developed using bulk properties of GaAs, we can conclude that it still seems to work quite well for flat surfaces, getting results similar to ab initio

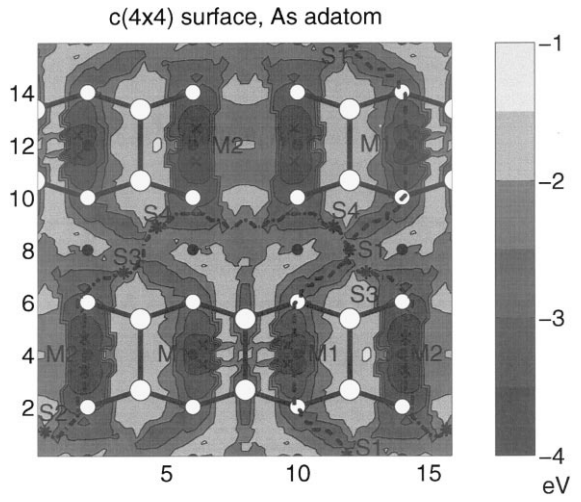

Fig. 9. The surface potential (with minima, saddle points and main diffusion paths) of the c(4×4) reconstruction for an arsenic adatom.

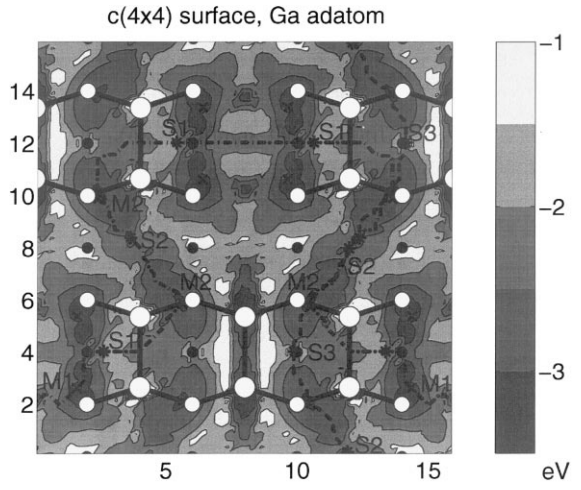

Fig. 10. The surface potential (with minima, saddle points and main diffusion paths) of the c(4×4) reconstruction for a gallium adatom.

calculations. Therefore it may be expected to give useful information about the large-scale step structures which have so far been too complicated to study with ab initio methods.

4.3. Adiabatic potentials for stepped surfaces

The adiabatic potential energy surfaces for the A step are seen in Figs. 11 and 12, with the corresponding minima and saddle points given in Table 8. For the B step, the energy surfaces are seen in Figs. 13 and 14, and the corresponding minima and saddle points in Table 9.

For these step structures, the main diffusion energy barriers E_D have been collected in Tables 10 and 11. In both cases, the diffusion barrier along the step is for a diffusion path near the step edge on the lower layer. The diffusion across the step is divided into cases *step down* for diffusion from a minimum on the higher layer to a minimum on the lower layer and *step up* for diffusion from a minimum on the lower layer to a minimum on the higher layer.

The diffusion barriers in both cases can be compared with the diffusion barriers on flat surfaces. For the arsenic adatom (Table 10), we have a diffusion barrier along the A step which is 0.15 eV smaller than the diffusion barrier in the

Table 6
Minima and saddle points on the c(4×4) surface

	Label	Energy (eV)	
		As	Ga
Minima	M1	−3.96	−3.12
	M2	−3.87	−3.04
Saddle points	S1	−2.41	−1.96
	S2	−2.20	−2.41
	S3	−2.26	−2.32
	S4	−2.26	–

Table 7
Diffusion barriers for gallium and arsenic adatoms on the most common reconstructed surfaces

Surface	Adatom	Direction	E_D (eV)
β2(2×4)	As	(110)	1.6
		$(\bar{1}10)$	1.5
	Ga	(110)	2.1
		$(\bar{1}10)$	1.7
β(2×4)	As	(110)	1.6
		$(\bar{1}10)$	1.5
	Ga	(110)	2.0
		$(\bar{1}10)$	1.9
c(4×4)	As	(110)	1.55
		$(\bar{1}10)$	1.7
	Ga	(110)	0.8
		$(\bar{1}10)$	1.15

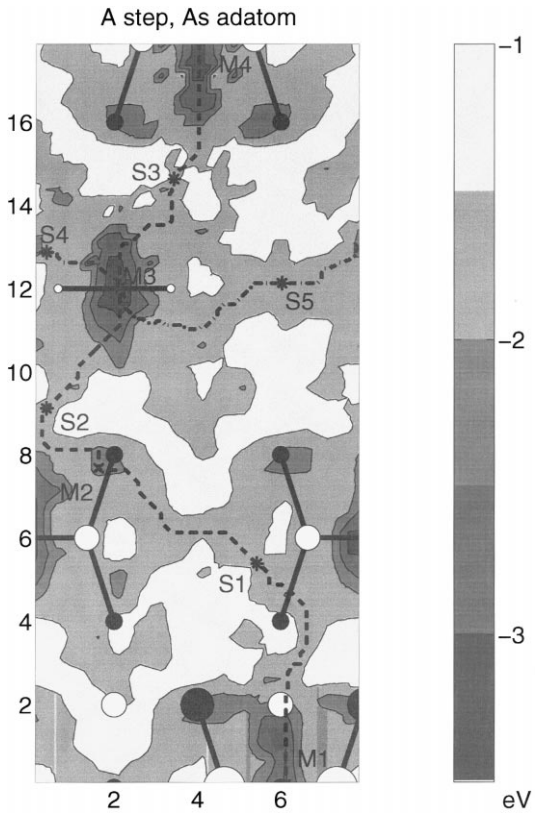

Fig. 11. The adiabatic potential surface of the A-β2(2×4) surface step for an arsenic adatom.

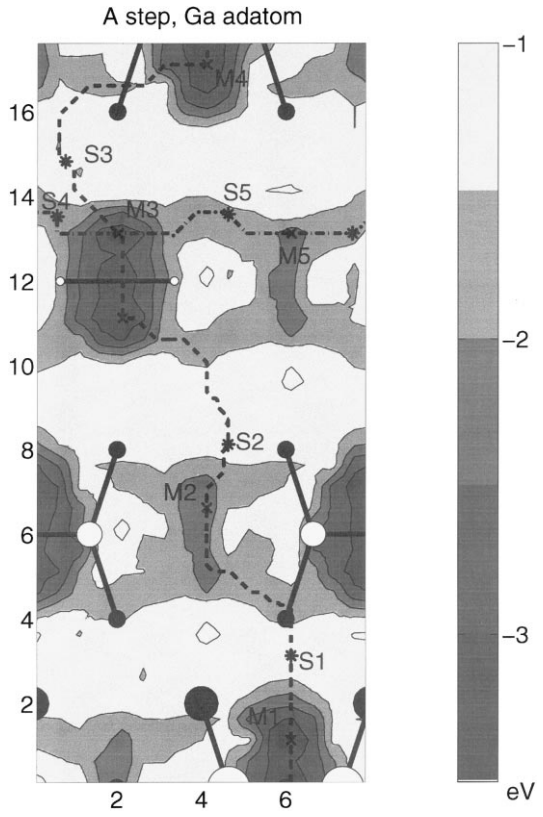

Fig. 12. The adiabatic potential surface of the A-β2(2×4) surface step for a gallium adatom.

same direction on the flat surface. It is also approximately equal to the the diffusion barrier for diffusion across the step in both directions, as well as in the same direction on a flat surface. The A step is therefore not expected to function as a nucleation site for arsenic adatoms. Neither is there any evidence for the existence of a step-edge barrier in going down the step, the diffusion barrier for diffusion down from a higher terrace actually being 0.1 eV less than the diffusion barrier on a flat surface.

On the other hand, diffusion along the B step has a diffusion barrier that is 0.3 eV larger than diffusion on a flat surface, and 0.2 eV higher than diffusion away from the step (on the lower terrace). In addition to this, the minima at the B step are approximately 0.1 eV lower than the minima on the flat surface. This all suggests that the B step will function as a nucleation site for arsenic adatoms. There is, once again, no evidence of a step-edge barrier, although diffusion from a lower terrace is slightly (0.1 eV) more difficult.

Table 8
Minima and saddle points on the A step

	Label	Energy (eV)	
		As	Ga
Minima	M1	−3.06	−3.29
	M2	−2.11	−2.41
	M3	−3.13	−3.31
	M4	−3.06	−3.25
	M5	–	-2.31
Saddle points	S1	−1.56	−1.27
	S2	−1.61	−1.28
	S3	−1.54	−1.27
	S4	−1.76	−1.65
	S5	−1.65	−1.69
	S6	–	−1.65

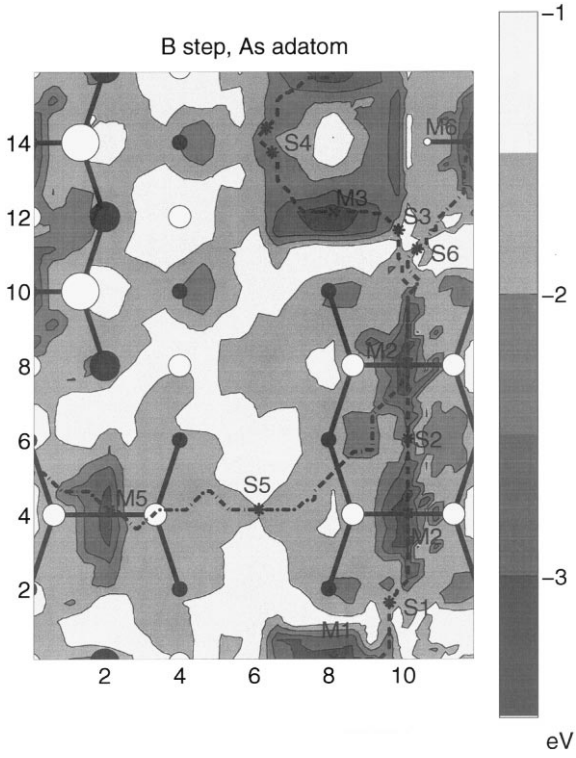

Fig. 13. The adiabatic potential surface of the B-β2(2×4) surface step for an arsenic adatom.

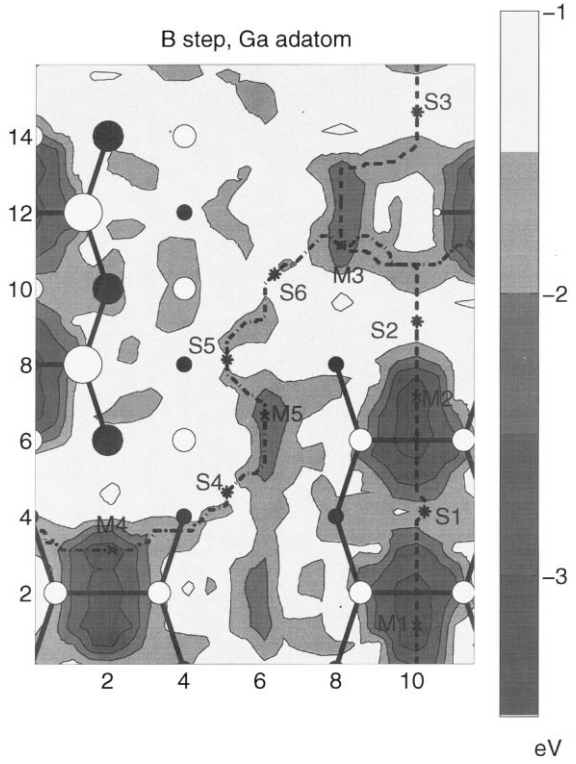

Fig. 14. The adiabatic potential surface of the B-β2(2×4) surface step for a gallium adatom.

For the gallium adatom (Table 11), which is the more interesting one from the point of view of MBE growth, there is evidence for the existence of an extra barrier, although only for the B-type step. The results show evidence of a additional 0.25 eV barrier on going down the B step, as well as somewhat faster diffusion along the step (0.10 eV difference in diffusion barriers as compared with the flat surface). For the A type of step, diffusion along the step is slightly easier (a diffusion barrier difference of 0.05 eV compared with the flat surface), but there is no evidence for the existence of a step-edge barrier. For the gallium adatoms, there is no appreciable difference in the diffusion along the different step types and consequently no evidence for different step-edge characteristics seen in STM images, where elongated islands can be seen to form on nominally smooth surfaces [14]. In these islands the A-type steps are long and relatively smooth while the B-type steps are jagged and exhibit a large number of kinks.

Table 9
Minima and saddle points on the B step

	Label	Energy (eV)	
		As	Ga
Minima	M1	−3.24	−3.24
	M2	−3.06	−3.29
	M3	−3.23	−2.58
	M4	–	−3.29
	M5	−3.13	−2.29
	M6	−3.13	–
Saddle points	S1	−1.59	−1.64
	S2	−2.16	−1.28
	S3	−1.59	−1.26
	S4	−2.06	−1.45
	S5	−1.54	−1.45
	S6	−1.54	−1.37

Neither of the adatoms nor the step types show evidence of a lower-energy minimum near the step edge which could trap the adatoms on the step

Table 10
Diffusion barriers for arsenic adatoms in the vicinity and across the A and B types of step

Type	Direction	E_D (eV)
A	Along step ($\bar{1}10$)	1.45
	Flat surface ($\bar{1}10$)	1.6
	Step down (110)	1.4
	Step up (110)	1.5
	Flat surface (110)	1.5
B	Along step (110)	1.8
	Flat surface (110)	1.5
	Step down ($\bar{1}10$)	1.6
	Step up ($\bar{1}10$)	1.7
	Flat surface ($\bar{1}10$)	1.6

Table 11
Diffusion barriers for gallium adatoms in the vicinity and across the A and B types of step

Type	Direction	E_D (eV)
A	Along step ($\bar{1}10$)	1.65
	Flat surface ($\bar{1}10$)	1.7
	Step down (110)	2.05
	Step up (110)	2.05
	Flat surface (110)	2.1
B	Along step (110)	2.0
	Flat surface (110)	2.1
	Step down ($\bar{1}10$)	1.95
	Step up ($\bar{1}10$)	1.95
	Flat surface ($\bar{1}10$)	1.7

edge. This is due to the fact that the main energy minima are still at the short-bridge sites between surface dimer arsenic atoms, and this is not appreciably modified by the proximity of the edge, at least in the present model.

Our calculations do not directly support the formation of smooth A-type steps and ragged B-type steps, which is observed experimentally [67–69]. For the gallium adatom, diffusion is faster along the step edge for both the A- and B-type steps as compared with the flat surface. Additionally, there are no deep minima near the steps to function as nucleation sites for diffusing adatoms. Likewise, the potential shows no evidence for the elongation of islands along the A step direction, which is another effect seen experimentally [15].

Several studies have been published for the diffusion of gallium on GaAs(001) surfaces. These include both experimental RHEED measurements, as well as ab initio calculations. These calculations have resulted in a several estimates of the diffusion barriers E_D, shown in Table 12. In the case of ab initio calculations, the diffusion constants have been evaluated in a direction parallel to the dimers as well as perpendicular to them. For these results, the ratios between E_D in different directions are also shown in the table.

The work of Ohta [72] was the first to examine the possible diffusion anisotropy in the GaAs(001) surface. They found no difference in the energy barriers, estimating both to be 2.8 eV, but they found the ratio of diffusion prefactors to be 4:1 in favor of diffusion in the ($\bar{1}10$) direction, which is also the preferred direction in ab initio calculations.

Ab initio studies have been performed for the $\beta(2\times4)$ [64] and $\beta2(2\times4)$ [65] structures. Both of these studies have mapped the adiabatic potential energy surface of the (2×4) reconstruction and calculated the diffusion paths and diffusion energy barriers from that. The results produced by our MD simulations basically agree with the ab initio calculations. The ($\bar{1}10$) direction of top arsenic dimers is the direction of fastest diffusion in all these cases.

Unlike for the (001) surface of silicon, where the formation of long dimer chains on the surface causes a clear anisotropy in the diffusion potential,

Table 12
Summary of the diffusion barriers and anisotropies for gallium adatoms on the GaAs(001) surface

E_D(eV)	Ratio	Method	Surface	Reference
1.3	–	RHEED	(2×4)	[70]
4.0	–	RHEED	(1×1)	[71]
2.8	–	RHEED	(2×4)	[72]
1.5 (110) 1.2 ($\bar{1}10$)	1.25	ab initio	$\beta2(2\times4)$	[65]
1.05 (110) 0.85 ($\bar{1}10$)	1.24	ab initio	$\beta(2\times4)$	[64]
2.15 (110) 1.70 ($\bar{1}10$)	1.26	MD	$\beta2(2\times4)$	Present work
1.95 (110) 1.85 ($\bar{1}10$)	1.05	MD	$\beta(2\times4)$	Present work

the effects are less clear for the GaAs surface, as well as favoring the dimer direction instead of the perpendicular dimer-row direction. The missing dimer rows hinder diffusion along the direction perpendicular to the dimers. Estimating from the β surface potential, the diffusion barrier between adjacent minima on a hypothetical (2×1) dimer-row surface would be 0.9 eV for an arsenic adatom and 1.35 eV for a gallium adatom, compared with 1.5 eV and 1.85 eV, respectively, in the direction of the dimers. Simple electron-counting heuristics, however, disallow such a structure for GaAs, and no evidence for its existence has surfaced. This suggests that, like in the ab initio studies [64,65], the smaller diffusion constant in the (110) direction is caused mainly by the missing arsenic dimers in the reconstructed surface.

5. Conclusions

We have in this work determined the adiabatic surface potentials for arsenic and gallium adatoms on some important smooth and stepped GaAs(001) surfaces. The results for the flat surface reconstructions suggest that the Tersoff potential can give reasonably reliable results for surface energetics. The stability calculations give results similar to ab initio studies, and the potential surface minima are also found in the same places – the short-bridge sites in the middle of surface dimers. In the calculations for steps, the results for an gallium adatom suggest the existence of a step-edge barrier of about 0.25 eV, although only for the B-type step. The effective step-edge barrier from the experiments of MBE growth has been estimated to be about 0.06 eV or larger [5,7], which in part may then be due to the presence of configurations corresponding to B-type steps. We also find that diffusion along both steps is slightly faster than on a flat surface, but there is no real difference between the two types of step, as would be expected by experimental results. For the arsenic adatom, no evidence supporting the existence of a step-edge barrier was found in this study, but there seems to be a diffusion anisotropy along the steps. Further experimental and theoretical studies of the microscopic nature of these surfaces and adatom dynamics on them would certainly be desirable.

Acknowledgements

We wish to thank Dr Tomi Mattila for providing us with the MD program code used here. This work was supported in part by the Academy of Finland.

References

[1] M. Lagally (Ed.), in: Kinetics of Ordering and Growth on Surfaces, Plenum Press, New York, 1990.
[2] D.J. Eaglesham, J. Appl. Phys. 77 (1995) 3597.
[3] C. Orme, M.D. Johnson, K.T. Leung, B.G. Orr, Mater. Sci. Eng. B 30 (1995) 143.
[4] J.E. Van Nostrand, S.J. Chey, D.G. Cahill, A.E. Botchkarev, H. Morkoc, Surf. Sci. 346 (1996) 136.
[5] J. Krug, Adv. Phys. 46 (1997) 139.
[6] J. Villain, J. Phys. I 1 (1991) 19.
[7] P. Smilauer, D.D. Vvedensky, Phys. Rev. B 52 (1995) 14263.
[8] T. Ala-Nissila, S.C. Ying, Progr. Surf. Sci. 39 (1992) 227.
[9] T. Ala-Nissila, S.C. Ying, Surf. Sci. Lett. 235 (1990) L341.
[10] G.H. Vineyard, Phys. Rev. 110 (1958) 999.
[11] L.Y. Chen, S.C. Ying, Phys. Rev. B 49 (1994) 13838.
[12] G. Erlich, F.G. Hudda, J. Chem. Phys. 44 (1966) 1039.
[13] R.L. Schwoebel, J. Appl. Phys. 40 (1969) 614.
[14] M.D. Pashley, K.W. Haberern, J.M. Gaines, Surf. Sci. 267 (1992) 153.
[15] E.J. Heller, M.G. Lagally, Appl. Phys. Lett. 60 (1992) 2675.
[16] E.J. Heller, Z.Y. Zhang, M.G. Lagally, Phys. Rev. Lett. 71 (1993) 743.
[17] M.D. Johnson, C. Orme, A.W. Hunt, D. Graff, J. Sudijono, L.M. Sander, B.G. Orr, Phys. Rev. Lett. 72 (1994) 116.
[18] J. Tersoff, Phys. Rev. Lett. 56 (1986) 632.
[19] J.R. Arthur, Surf. Sci. 43 (1974) 449.
[20] T.-C. Chiang, R. Ludeke, M. Aono, G. Landgren, F.J. Himpsel, D.E. Eastman, Phys. Rev. B 27 (1983) 4770.
[21] A.Y. Cho, J. Appl. Phys. 41 (1970) 2780.
[22] A.Y. Cho, J. Appl. Phys. 42 (1971) 2074.
[23] A.Y. Cho, J. Appl. Phys. 47 (1976) 2841.
[24] I. Kamiya, D.E. Aspnes, L.T. Florez, J.P. Harbison, Phys. Rev. B 46 (1992) 15894.
[25] J. Massies, P. Etienne, F. Dezaly, N.T. Linh, Surf. Sci. 99 (1980) 121.
[26] M.D. Pashley, Phys. Rev. B 40 (1989) 10481.
[27] M.D. Pashley, K.W. Haberern, W. Friday, J.M. Woodall, P.D. Kirchner, Phys. Rev. Lett. 60 (1988) 2176.

[28] M.C. Gallagher, R.H. Prince, R.F. Willis, Surf. Sci. 275 (1992) 31.
[29] T. Hashizume, Q.K. Xue, J. Zhou, A. Ichimiya, T. Sakurai, Phys. Rev. Lett. 73 (1994) 2208.
[30] T. Hashizume, Q.-K. Xue, A. Ichimiya, T. Sakurai, Phys. Rev. B 51 (1995) 4200.
[31] D.K. Biegelsen, R.D. Bringans, J.E. Northrup, L.-E. Swartz, Phys. Rev. B 41 (1990) 5701.
[32] L. Broekman, R. Leckey, J. Riley, B. Usher, B. Sexton, Surf. Sci. 331–333 (1995) 1115.
[33] L. Broekman, R.C.G. Leckey, J.D. Riley, A. Stampfl, B.F. Usher, B.A. Sexton, Phys. Rev. B 51 (1995) 17795.
[34] J. Zhou, Q. Xue, H. Chaya, T. Hashizume, T. Sakurai, Appl. Phys. Lett. 64 (1994) 583.
[35] J.E. Northrup, S. Froyen, Phys. Rev. B 50 (1994) 2015.
[36] S.B. Zhang, A. Zunger, Phys. Rev. B 53 (1996) 1343.
[37] P.K. Larsen, J.H. Neave, J.F. van der Veen, P.J. Dobson, B.A. Joyce, Phys. Rev. B 27 (1983) 4966.
[38] M. Sauvage-Simkin, R. Pinchaux, J. Massies, P. Calverie, N. Jedrecy, J. Bonnet, I.K. Robinson, Phys. Rev. Lett. 62 (1989) 563.
[39] A.R. Avery, D.M. Holmes, J. Sudijono, B.A. Joyce, Surf. Sci. 323 (1995) 91.
[40] T. Ohno, Phys. Rev. Lett. 70 (1993) 631.
[41] J.E. Northrup, S. Froyen, Phys. Rev. Lett. 71 (1993) 2276.
[42] S.B. Zhang, A. Zunger, Mater. Sci. Eng. B 30 (1995) 127.
[43] J. Tersoff, Phys. Rev. B 37 (1988) 6991.
[44] J. Tersoff, Phys. Rev. B 39 (1989) 5566.
[45] R. Smith, Nucl. Instrum. Meth. Phys. Res. B 67 (1992) 335.
[46] M. Sayed, J.M. Jefferson, A.B. Walker, A.G. Cullis, Nucl. Instrum. Meth. Phys. Res. B 102 (1995) 218.
[47] N. Moll, A. Kley, E. Pehlke, M. Scheffler, unpublished work.
[48] C. Roland, G.H. Gilmer, Phys. Rev. B 46 (1992) 13428.
[49] M. Tmar, A. Gabriel, C. Chatillon, I. Ansara, J. Cryst. Growth 69 (1984) 421.
[50] J.E. Northrup, S. Froyen, Mater. Sci. Eng. B 30 (1995) 81.
[51] G.-X. Qian, R.M. Martin, D.J. Chadi, Phys. Rev. Lett. 60 (1988) 1962.
[52] K. Sumitomo, H. Yamaguchi, Y. Hirota, T. Nishioka, T. Ogino, Surf. Sci. 355 (1996) L361.
[53] J.M. McCoy, U. Korte, P.A. Maksym, G. Meyer-Ehmsen, Surf. Sci. 261 (1992) 29.
[54] M. Witte, G. Meyer-Ehmsen, Surf. Sci. Lett. 326 (1995) L449.
[55] C. Xu, J.S. Burnham, R.M. Braun, S.H. Goss, N. Winograd, Phys. Rev. B 52 (1995) 5172.
[56] V. Bressler-Hill, M. Wassermeier, K. Pond, R. Maboudian, G.A.D. Briggs, P.M. Petroff, W.H. Weinberg, J. Vac. Sci. Technol. B 10 (1992) 1881.
[57] H. Xu, T. Hashizume, T. Sakurai, Jpn. J. Appl. Phys. 32 (1993) 1511.
[58] W.G. Schmidt, F. Bechstedt, Surf. Sci. 360 (1996) L473.
[59] H. Li, S.Y. Tong, Surf. Sci. 282 (1993) 380.
[60] S.A. Chambers, Surf. Sci. Lett. 248 (1991) L274.
[61] S.A. Chambers, Surf. Sci. 261 (1992) 48.
[62] K. Shiraishi, T. Ito, J. Cryst. Growth 150 (1995) 158.
[63] G.P. Srivastava, S.J. Jenkins, Phys. Rev. B 53 (1996) 12589.
[64] T. Ohno, K. Shiraishi, T. Ito, JRCAT International Wprkshop on Atomically Controlled Surface Processes, Tsukuba, Japan.
[65] A. Kley, M. Scheffler, in: M. Scheffler, R. Zimmermann (Eds.), Proc. 23rd Int. Conf. on the Physics of Semiconductors, World Scientific, Singapore, 1996, p. 1031.
[66] C.C. Matthai, G.A. Moran, Appl. Surf. Sci 123/124 (1998) 653.
[67] M. Kasu, N. Kobayashi, H. Yamaguchi, Appl. Phys. Lett. 63 (1993) 678.
[68] M.D. Pashley, K.W. Haberern, J.M. Gaines, Appl. Phys. Lett. 58 (1991) 406.
[69] K. Pond, A.C. Gossard, A. Lorke, P.M. Petroff, Mater. Sci. Eng. B. 30 (1995) 121.
[70] J.H. Neave, P.J. Dobson, B.A. Joyce, J. Zhang, Appl. Phys. Lett. 47 (1985) 100.
[71] J.M. Van Hove, P.I. Cohen, J. Cryst. Growth 81 (1987) 13.
[72] K. Ohta, T. Kojima, T. Nakagawa, J. Cryst. Growth 95 (1989) 71.